The porphyrin TMPyP4 inhibits elongation during the noncanonical translation of the FTLD/ALS-associated GGGGCC repeat in the *C9orf72* gene

Received for publication, March 27, 2021, and in revised form, August 15, 2021 Published, Papers in Press, August 25, 2021,
https://doi.org/10.1016/j.jbc.2021.101120

Kohji Mori[1,*], Shiho Gotoh[1], Tomoko Yamashita[1], Ryota Uozumi[1], Yuya Kawabe[1], Shinji Tagami[1], Frits Kamp[2], Brigitte Nuscher[2], Dieter Edbauer[3,4], Christian Haass[2,3,4], Yoshitaka Nagai[5,6], and Manabu Ikeda[1]

From the [1]Department of Psychiatry, Osaka University Graduate School of Medicine, Osaka, Japan; [2]Biomedical Center (BMC), Ludwig-Maximilians Universität München, Munich, Germany; [3]German Center for Neurodegenerative Diseases (DZNE), Munich, Germany; [4]Munich Cluster for System Neurology (SyNergy), Munich, Germany; [5]Department of Neurotherapeutics, Osaka University Graduate School of Medicine, Osaka, Japan; and [6]Department of Neurology, Kindai University Faculty of Medicine, Osaka, Japan

Edited by Karin Musier-Forsyth

GGGGCC (G_4C_2) repeat expansion in the *C9orf72* gene has been shown to cause frontotemporal lobar degeneration and amyotrophic lateral sclerosis. Dipeptide repeat proteins produced through *r*epeat-*a*ssociated *n*on-AUG (RAN) translation are recognized as potential drivers for neurodegeneration. Therefore, selective inhibition of RAN translation could be a therapeutic avenue to treat these neurodegenerative diseases. It was previously known that the porphyrin TMPyP4 binds to G_4C_2 repeat RNA. However, the consequences of this interaction have not been well characterized. Here, we confirmed that TMPyP4 inhibits *C9orf72* G_4C_2 repeat translation in cellular and in *in vitro* translation systems. An artificial insertion of an AUG codon failed to cancel the translation inhibition, suggesting that TMPyP4 acts downstream of non-AUG translation initiation. Polysome profiling assays also revealed polysome retention on G_4C_2 repeat RNA, along with inhibition of translation, indicating that elongating ribosomes stall on G_4C_2 repeat RNA. Urea-resistant interaction between G_4C_2 repeat RNA and TMPyP4 likely contributes to this ribosome stalling and thus to selective inhibition of RAN translation. Taken together, our data reveal a novel mode of action of TMPyP4 as an inhibitor of G_4C_2 repeat translation elongation.

A hexanucleotide expansion in intron of *C9orf72* is a most common genetic cause of genetically inherited frontotemporal lobar degeneration (FTLD) and amyotrophic lateral sclerosis (ALS) (1–3). The disease-causing repeat expansion is transcribed into sense GGGGCC (G_4C_2) and antisense CCCCGG directions. Repeat RNAs bind to or even sequester a list of RNA-binding proteins (4–6). Moreover, we and others found that these RNA repeats are translated into five distinct dipeptide repeat (DPR) proteins, namely poly-(glycine alanine: GA), poly-(glycine proline: GP), poly-(glycine arginine: GR), poly-(proline alanine), and poly-(proline arginine) (7–11) through *r*epeat *a*ssociated *n*on-AUG (RAN) translation (12).

Widespread deposition of DPRs has been established as a specific neuropathological hallmark of *C9orf72*-related FTLD/ALS (13–15). Poly-GP is even detected in cerebrospinal fluid, and it is a disease state maker for carriers of *C9orf72* repeats that may be useful as a pharmacodynamic marker for clinical trials (16, 17). Importantly, recent studies have pointed out that poly-GR correlates with the severity of TDP-43 pathology and neurodegeneration (18–21). Moreover, multiple models expressing DPRs have shown neurodegenerative phenotypes (22–31).

Postulated mechanisms of DPR toxicity include dysregulated nucleocytoplasmic transport, cytoplasmic RNA transport, stress granule assembly/disassembly, translation, protein degradation, and RNA metabolism (27, 32–39). Although repeat-mediated lysosomal dysfunction because of reduced levels of C9orf72 protein presumably also contributes to the disease (40–42), accumulating reports support the notion that DPR toxicity could be a primary driver for the neurodegeneration in *C9orf72* FTLD/ALS. Therefore, inhibition of DPR expression would be an attractive therapeutic option for FTLD/ALS patients carrying *C9orf72* repeats. While the general mechanism of RAN translation remains elusive, RAN translation in the poly-GA frame of the *C9orf72* G_4C_2 repeat is probably initiated at a near cognate CUG codon 5′ upstream to the G_4C_2 repeat (42–45). Moreover, RAN translation is stimulated through cellular stress that corresponds with the levels of phosphorylated eukaryotic initiation factor 2α (43, 46–48). Interestingly, RNA helicase DDX3X has recently been proposed as a repressor of RAN translation of G_4C_2 repeat (49).

G_4C_2 repeat RNA forms RNA G-quadruplex structure (50, 51). A cationic porphyrin TMPyP4 is known to interact with G-quadruplex from G_4C_2 repeat RNA (52). Zhang *et al.* (53) previously reported that TMPyP4 mitigates G_4C_2 repeat–dependent neurotoxicity in *Drosophila* by suppressing hexanucleotide repeat–mediated nuclear import deficits by altering the structure of the repeat RNA. Moreover, TMPyP4 impedes G_4C_2 RNA granule formation (54). Recently, compound screening studies found that G-quadruplex–binding

* For correspondence: Kohji Mori, kmori@psy.med.osaka-u.ac.jp.

compounds including TMPyP4 inhibit RAN translation (55, 56); however, the detailed mechanism underlying the selective translation inhibition remains obscure. Using cellular models and *in vitro* assays of *C9orf72* FTLD/ALS, here we show that TMPyP4 selectively inhibits repeat translation at the elongation step.

Results

TMPyP4 inhibits poly-GA expression without affecting expression or nucleocytoplasmic distribution of G_4C_2 repeat RNA

To examine if TMPyP4 affects G_4C_2 repeat translation, we transfected a $(G_4C_2)_{80}$ expression plasmid, which encodes 80 repeats of G_4C_2 under the control of the elongation factor 1 (EF1) promoter into HeLa cells (Fig. 1*A*) (10, 38). The vector contains 113 base pairs of 5′ flanking region of the expanded G_4C_2 repeat including the near cognate CUG codon in poly-GA frame (42–45) and multiple stop codons but lacks ATG initiation codons in all reading frames. This allows quantitative monitoring of poly-GA expression from RAN translation (10, 38). Treatment of repeat transfected cells with increasing doses of TMPyP4 dramatically inhibited poly-GA expressions (Fig. 1, *B* and *C*). Corresponding RT-quantitative PCR (qPCR) analysis revealed that G_4C_2 repeat RNA expression was largely unaffected up to 20 μM of TMPyP4 (Fig. 1*D*). Thus, we choose 20 μM of TMPyP4 as a dose for most of the following cellular analysis. Aforementioned results suggest that TMPyP4 inhibits poly-GA expression without primarily affecting repeat transcription.

For efficient translation, nuclear export of the RNA transcript into the cytoplasm is necessary. Therefore, we next asked if TMPyP4 affects intracellular localization of the repeat RNA. A quantitative fluorescent *in situ* hybridization analysis was not feasible since TMPyP4 as well as the other porphyrins absorb and emit broad spectrum of light. Therefore, we performed biochemical separation of cytoplasmic and nuclear RNA of the repeat transfected cells. RT-qPCR analysis revealed more than 80% of nuclear-enriched long noncoding RNA MALAT1 transcript was found in nuclear-enriched fraction. Conversely, 60 to 70% of β-actin and GAPDH mRNA were found in the cytoplasm fraction where mRNA is normally enriched. These results ensure successful separation of cytoplasm and nuclear RNA in our experimental condition (Fig. 1*E*). In the same setting, about 70% of G_4C_2 repeat RNA accumulated in the nuclear-enriched fraction (Fig. 1*E*). Importantly, treatment with 20 μM TMPyP4 did not alter the nuclear/cytoplasmic distribution of G_4C_2 repeat RNA and the other tested transcripts (Fig. 1*E*). These results implicate that TMPyP4 suppresses poly-GA production possibly by inhibiting translation but not transcription or nucleocytoplasmic RNA export.

TMPyP4 inhibits G_4C_2 repeat translation in all reading frames but spares global translation

We next asked whether TMPyP4 blocks the expressions of the other DPRs. To do so, we applied previously developed cytomegalovirus (CMV) promoter-driven $(G_4C_2)_{80}$ repeat plasmids, which allow detectable expressions of poly-GA, poly-GP, and poly-GR using anti-FLAG antibodies (Fig. 2*A*). Dot blot analysis revealed that TMPyP4 treatment significantly reduced the expression of all the DPRs from G_4C_2 repeats (Fig. 2, *B* and *C*). These results indicate that

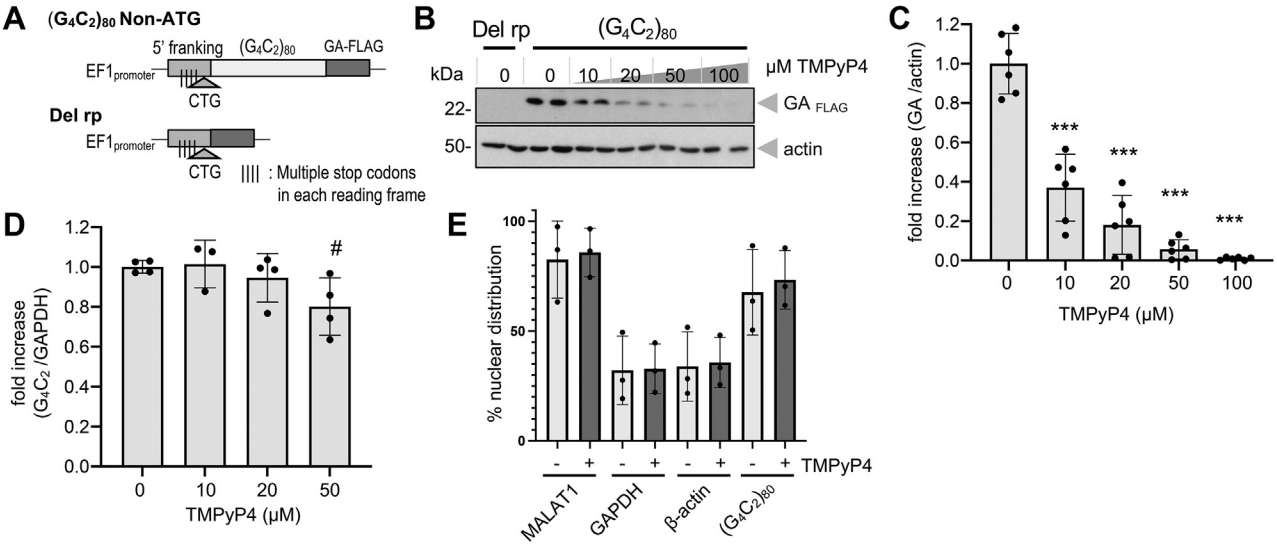

Figure 1. TMPyP4 inhibits RAN translation in a cellular model of *C9orf72* repeat expansion without affecting expression and localization of G_4C_2 repeat RNA. *A*, schema for $(G_4C_2)_{80}$ repeat plasmid and repeat deletion "Del rp" plasmid. Both share multiple stop codon containing 5′ flanking region of the expanded *C9orf72* G_4C_2 repeat. *B* and *C*, increasing doses of TMPyP4 significantly inhibit poly-GA expression in $(G_4C_2)_{80}$ transfected HeLa cells. n = 3, experiments performed in duplicates. ANOVA with Dunnett post hoc test *versus* "0." ***$p < 0.0001$. *D*, treatment with increasing doses of TMPyP4 gives modest inhibition on repeat RNA expression levels in RT-quantitative PCR. n = 2, experiments performed in duplicates. ANOVA with Dunnett post hoc test *versus* "0." #$p = 0.0708$. *E*, percent of nuclear distribution of MALAT-1, GAPDH, β-actin, and G_4C_2 repeat RNA of cells cultured in the presence (+) or the absence (–) of 20 μM TMPyP4. TMPyP4 does not significantly affect the percent of nuclear distributions of these RNA. n = 3. Two-tailed paired *t* test. All graphs are shown as mean ± SD. Each dot represents single data point. GA, glycine alanine; G_4C_2, GGGGCC; RAN, *r*epeat-*a*ssociated *n*on-AUG.

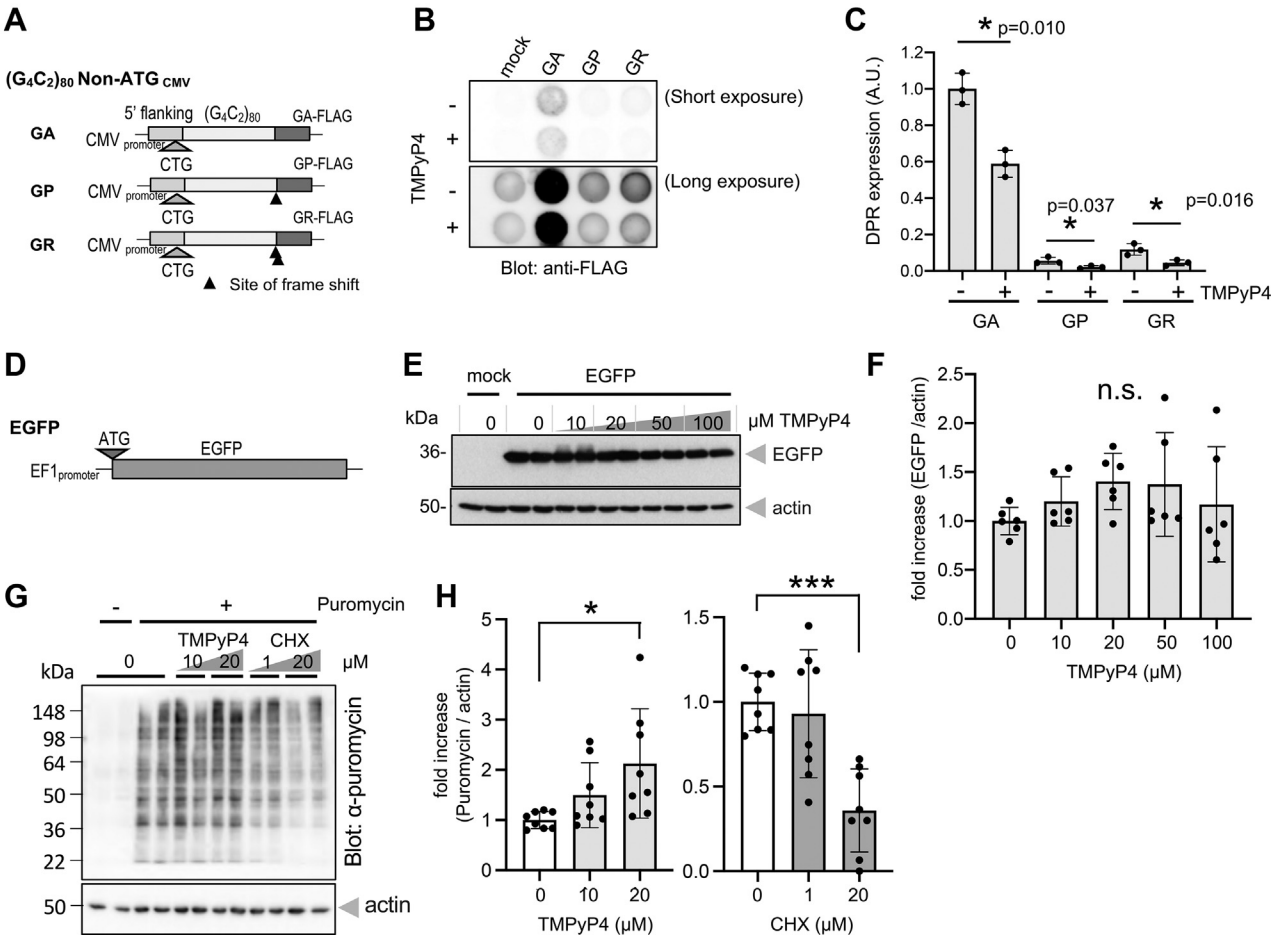

Figure 2. TMPyP4 inhibits RAN translation of *C9orf72* expanded G_4C_2 repeat in all reading frames but spares global cellular translation. *A*, schema of strong CMV promoter-driven $(G_4C_2)_{80}$ plasmids lacking ATG initiation codon. With artificial frame shift insertion before C-terminal FLAG tag, each plasmid labels one DPR (GA, GP, or GR) with FLAG tag. *B* and *C*, dot blot analysis of cells transfected with repeat plasmid (*A*) or mock plasmid cultured for two overnights in the presence (+) or the absence (−) of 20 μM TMPyP4. n = 3. Two-tailed paired *t* test. *D*, schematic representation of an EF1 promoter-driven EGFP expression plasmid containing conventional ATG initiation codon. *E* and *F*, no inhibition of cellular EGFP expression with increasing doses of TMPyP4. n = 3, experiments performed in duplicates. ANOVA with Dunnett post hoc test *versus* "0." *G*, puromycin incorporation assay monitoring active cellular translation. Cells were treated with/without TMPyP4 or CHX and then pulse labeled with puromycin. Actively translating proteins during pulse labeling (*i.e.*, proteins incorporated puromycin) were visualized with antipuromycin antibody. β-actin blot is shown as loading control. *H*, signal intensities of each lane of puromycin blot were measured and normalized with corresponding β-actin signals. While translation inhibitor CHX suppressed global translation, TMPyP4 significantly enhanced puromycin incorporation. n = 4, experiments performed in duplicates. ANOVA with Dunnett post hoc test *versus* "0" in each compound. Data points "0" in these two graphs show same data. **p* = 0.0112 and ****p* = 0.0003. All graphs are shown as mean ± SD. Each dot represents single data point. CHX, cycloheximide; CMV, cytomegalovirus; DPR, dipeptide repeat; EF1, elongation factor 1; EGFP, enhanced GFP; GA, glycine alanine; G_4C_2, GGGGCC; GP, glycine alanine; GR, glycine arginine; RAN, *r*epeat-*a*ssociated *n*on-AUG.

TMPyP4 inhibits DPR productions from G_4C_2 repeat in all reading frames.

Our next question was whether the inhibitory effect of TMPyP4 is selective for repeat translation. In clear contrast to poly-GA expression, treatment with up to 100 μM of TMPyP4 did not significantly inhibit cellular enhanced GFP (EGFP) expressions from conventional AUG-initiated translation (Fig. 2, *D*–*F*). To extend the observation in single reporter protein into global translation, a puromycin incorporation assay was performed (57). Puromycin is an analog of aminoacyl-tRNA, which is incorporated into newly synthesized polypeptide chain. Accordingly, signal intensities from puromycin-labeled proteins are proportional to global translation efficacy. When cells were treated with cycloheximide (CHX), an established translation inhibitor, signals from puromycin-labeled proteins detected with anti-puromycin antibody were significantly reduced (Fig. 2, *G* and *H*). In clear contrast, cells treated with TMPyP4 did not show any sign of global translation inhibition (Fig. 2, *G* and *H*). These results suggest that TMPyP4 selectively inhibits poly-GA expression while sparing global translation.

TMPyP4 is not a selective inhibitor of non-AUG initiation of RAN translation

Since TMPyP4 inhibited non-AUG–dependent G_4C_2 repeat translation (RAN translation), but not conventional AUG-dependent translation of EGFP and puromycin-labeled global translation, we asked whether the effect of TMPyP4 on G_4C_2 repeat would be cancelled with artificial insertion of AUG initiation codon. Therefore, a Kozak sequence with ATG codon was introduced just upstream of the hexanucleotide

repeat in the poly-GA reading frame (ATG-$(G_4C_2)_{80}$) (Fig. 3*A*). In transfected cells, this plasmid allowed robust expression of the poly-GA-FLAG protein *via* conventional translation. Unexpectedly, TMPyP4 also inhibited this AUG-dependent poly-GA expression in a dose-dependent manner (Fig. 3, *B* and *C*). These results imply that TMPyP4 is not a selective inhibitor of non-AUG initiation, but it still selectively inhibits G_4C_2 repeat translation.

Preferential inhibition of G_4C_2 repeat translation by TMPyP4 regardless of AUG initiation or non-AUG initiation in an in vitro *translation assay*

To exclude indirect effects of TMPyP4 on $(G_4C_2)_{80}$ expression, we tested its potency using *in vitro* translation assays with rabbit reticulocyte lysates and *in vitro* transcribed RNA. 5′cap containing repeat RNA and control RNA were synthesized in *in vitro* transcription followed by 3′ polyadenylation (Fig. 4*A*). Subsequent *in vitro* translation assays revealed a dose-dependent inhibition of poly-GA translation irrespective of the absence or the presence of an AUG codon (Fig. 4*B*, *top and middle panels*, and *C*). In the cell-free system, TMPyP4 was effective at lower concentration. Consistent with the results in our cellular model (Fig. 2, *D–F*), translation inhibition was less prominent on EGFP (Fig. 4*B*, *lower panel* and *C*). These results further support the notion that TMPyP4 selectively and directly inhibits G_4C_2 repeat translation regardless of AUG initiation or non-AUG initiation.

TMPyP4 causes inefficient elongation and ribosome stalling on G_4C_2 repeat RNA

Next, we asked if elongation step is the target of TMPyP4 for the selective inhibition of repeat translation. To test this possibility, we performed a polysome profiling assay (Fig. 5*A*). Inefficient translation elongation is known to cause the retention of multiple ribosomes (polysomes) on a mRNA molecule (58). Repeat transfected HeLa cells were cultured overnight in the presence or the absence of TMPyP4 and then treated with CHX for 3 min to acutely halt elongation. Cytoplasmic fraction of the cells was then loaded on the top of the 7 to 47% linear sucrose gradient. After ultracentrifugation, fractions were sequentially isolated from the top of the gradient (59). Polysome profiles were monitored through an absorbance at 260 nm (Fig. 5*B*). In a polysome profiling assay, it has already been established that 40S, 60S, monosome, and polysome elute in that order. To better allocate the elution profile to 40S, 60S ribosome and monosome in our assay, we purified RNA contained in each of fraction (fr.) 4 to 7 and performed bioanalyzer analysis (Fig. 5*C*). This analysis allowed us to automatically monitor rRNA ratio (28S/18S, *e.g.*, non-fractionated total RNA from HeLa cell showed (28S/18S) ratio of 2.6 [Fig. 5*C*, *the lowest panel*]). 40S ribosome and 60S ribosome contain 18S rRNA and 28S rRNA, respectively, and monosome has both rRNA species theoretically at the approximate ratio of 1:2.7 in bioanalyzer analysis. Since fr. 4 contained only 18S rRNA, 40S ribosome is enriched in this fraction. Similarly, 28S rRNA-enriched fr. 6 corresponds to 60S ribosome-enriched fraction. Accordingly, we interpret that fr. 5 is in transition of 40S- and 60S-enriched elution and fr. 7 corresponds to monosome-enriched fraction (Fig. 5, *B* and *C*). Then, RT-qPCR analysis targeting G_4C_2 repeat RNA was performed on the combined 40S + 60S + monosome fractions (fr. 4–8), low-weight polysome fractions (fr. 9–13), and high-weight polysome fractions (fr. 14–22) (Fig. 5*B*). Although TMPyP4 globally induced slight shift toward increased absorbance at 260-nm signals in the combined 40S + 60S+ monosome fractions and decreased absorbance at 260-nm signals in high-weight polysome fractions (Fig. 5*B*), TMPyP4 treatment induced significant retention of G_4C_2 repeat RNA in the high-weight polysome fractions as determined by RT-qPCR (Fig. 5*D*). To reveal more detailed distribution of G_4C_2 repeat RNA in the polysome profiling assay, we monitored the relative abundance of G_4C_2 repeat RNA in each fraction of the sucrose gradients of TMPyP4-treated or untreated cells (Fig. 5*E*). This revealed repeat RNA is especially enriched in heaviest fractions (fr. 21 and 22) of TMPyP4-treated cells when compared with that of TMPyP4-untreated cells (Fig. 5*E*). Along with selective inhibition of G_4C_2 repeat translation, these results suggest that TMPyP4 caused inefficient

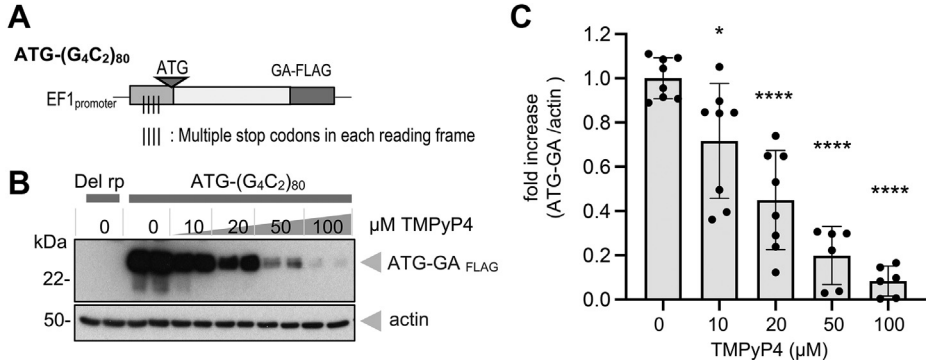

Figure 3. TMPyP4 inhibits not only non-AUG-dependent but AUG-dependent G_4C_2 repeat translation in cells. *A*, schema for $(G_4C_2)_{80}$ repeat plasmid with artificial insertion of good Kozak sequence with conventional ATG initiation codon in poly-GA frame. *B* and *C*, increasing doses of TMPyP4 significantly inhibit poly-GA expression in ATG-$(G_4C_2)_{80}$ transfected cells. n = 4 (or three in 50 and 100 μM). Experiments performed in duplicates. ANOVA with Dunnett post hoc test *versus* "0." *p = 0.0125 and ****$p < 0.0001$. Graphs are shown as mean ± SD. Each dot represents single data point. GA, glycine alanine; G_4C_2, GGGGCC.

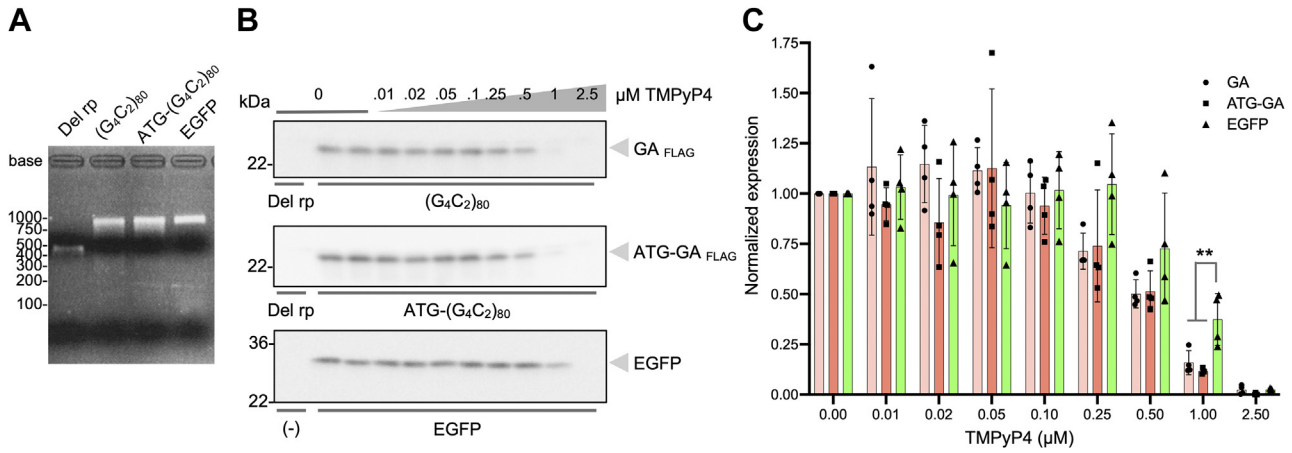

Figure 4. TMPyP4 preferentially inhibits G_4C_2 repeat translation regardless of AUG initiation or non-AUG initiation in *in vitro* translation assay. *A*, formaldehyde denaturing gel electrophoresis of purified *in vitro*–transcribed RNA with 5′ cap and 3′ polyadenylation. *B* and *C*, Western blot analysis of samples from *in vitro* translation with rabbit reticulocyte lysates in the presence or the absence of increasing doses of TMPyP4. Quantifications are shown in *C*. Four independent experiments. One-way ANOVA with Tukey post hoc test. $^{**}p = 0.0091$ (EGFP *versus* GA) or $p = 0.0030$ (EGFP *versus* ATG-GA). Graphs are shown as mean ± SD. Each dot represents single data point. EGFP, enhanced GFP; GA, glycine alanine; G_4C_2, GGGGCC.

elongation and thus stalling of multiple ribosomes selectively on G_4C_2 repeat RNA.

TMPyP4 induces urea-resistant electromobility shift on G_4C_2 repeat RNA

Our next question was the mechanism how TMPyP4 inhibits elongation in repeat RNA translation. One plausible explanation is that tight and direct interactions between TMPyP4 and G_4C_2 repeat RNA hinder efficient elongation. To test the hypothesis, we performed EMSA. Either synthetic 5′ FAM (fluorescein)-labeled RNA containing eight repeats of G_4C_2 repeats or 5′ FAM-labeled 49 nucleotides synthetic RNA called generic RNA (60, 61), a control RNA oligonucleotide, which is originally adopted from pcDNA3 polylinker sequence, was mixed with TMPyP4 and electrophoresed in non-denaturing condition. With increasing TMPyP4 dosages, FAM signals from both generic and G_4C_2 repeat RNA shifted toward higher molecular weight suggesting the presence of substantial interactions between not only G_4C_2 RNA–TMPyP4 but also generic RNA–TMPyP4 (Fig. 6, *A* and *B*, *side bars of upper panels*). FAM signals were quenched at higher doses of TMPyP4, possibly because TMPyP4 absorbs part of emitted light from FAM. When the same RNA–TMPyP4 mixtures were run on denaturing gels containing 6.5 M urea, the upper shifts of generic RNA–TMPyP4 complex were mostly abolished, and consistent FAM signals were obtained irrespective of the doses of TMPyP4 (Fig. 6*B*, *lower panel*). These results indicate that generic RNA–TMPyP4 complexes are readily disrupted by denaturing urea. In clear contrast, the FAM-$(G_4C_2)_8$ signals consistently showed urea-resistant upper shift even at lowest dose of TMPyP4 (0.25 μM) (Fig. 6*A*, *lower panel*, *red arrowhead*). These results support the formation of urea-resistant rigid interaction between TMPyP4 with the G_4C_2 repeat RNA. Such a tight interaction could at least in part explain the mechanism of elongation inhibition on the G_4C_2 repeat RNA.

Discussion

Here, we revealed that the G-quadruplex–binding porphyrin TMPyP4 inhibits *C9orf72* G_4C_2 repeat translation at the elongation step. TMPyP4 had previously been reported to interact with G-quadruplex structure of G_4C_2 repeat RNA *in vitro* (52, 55, 62) and was recently shown to inhibit RAN translation of CGG triplet repeat in *in vitro* translation (55). However, effect of TMPyP4 on *C9orf72* G_4C_2 repeat RAN translation and its mechanism of action have not yet been described especially in a cell culture model.

At concentrations already effective in inhibiting DPR translation in cells, TMPyP4 has no apparent effect on repeat RNA expression or on its nuclear–cytoplasmic distribution. Similarly, no inhibition on cellular global translation was observed. Interestingly, an artificial insertion of conventional initiation codon on repeat RNA failed to abolish the inhibitory effect of TMPyP4 indicating that the prime target of TMPyP4 is not the non-AUG initiation of RAN translation. *In vitro* translation assays further confirmed that TMPyP4 preferentially inhibits repeat translation again irrespective of the presence or the absence of conventional initiation codon. Interestingly, Green *et al.* (55) recently reported that TMPyP4 as well as other G-quadruplex–binding compounds (anthralin and PPIX) inhibit not only non-AUG dependent but also AUG-dependent translation of CGG triplet repeat in an *in vitro* translation assay. Their finding for CGG repeats is very consistent with our results in G_4C_2 repeat of *C9orf72*.

TMPyP4 did not at all inhibit cellular EGFP expression and global translation; however, in the *in vitro* translation assay, there was weak but consistent inhibition of EGFP translation by TMPyP4. Such discrepancy may be explained by the differences in assay condition including protein concentrations, number of ribosomes working in translation, ionic strength, the presence or the absence of RNA-binding proteins such as ATP-dependent RNA helicase, which may easily clear nonspecifically bound TMPyP4 from the non-G-quadruplex forming RNA.

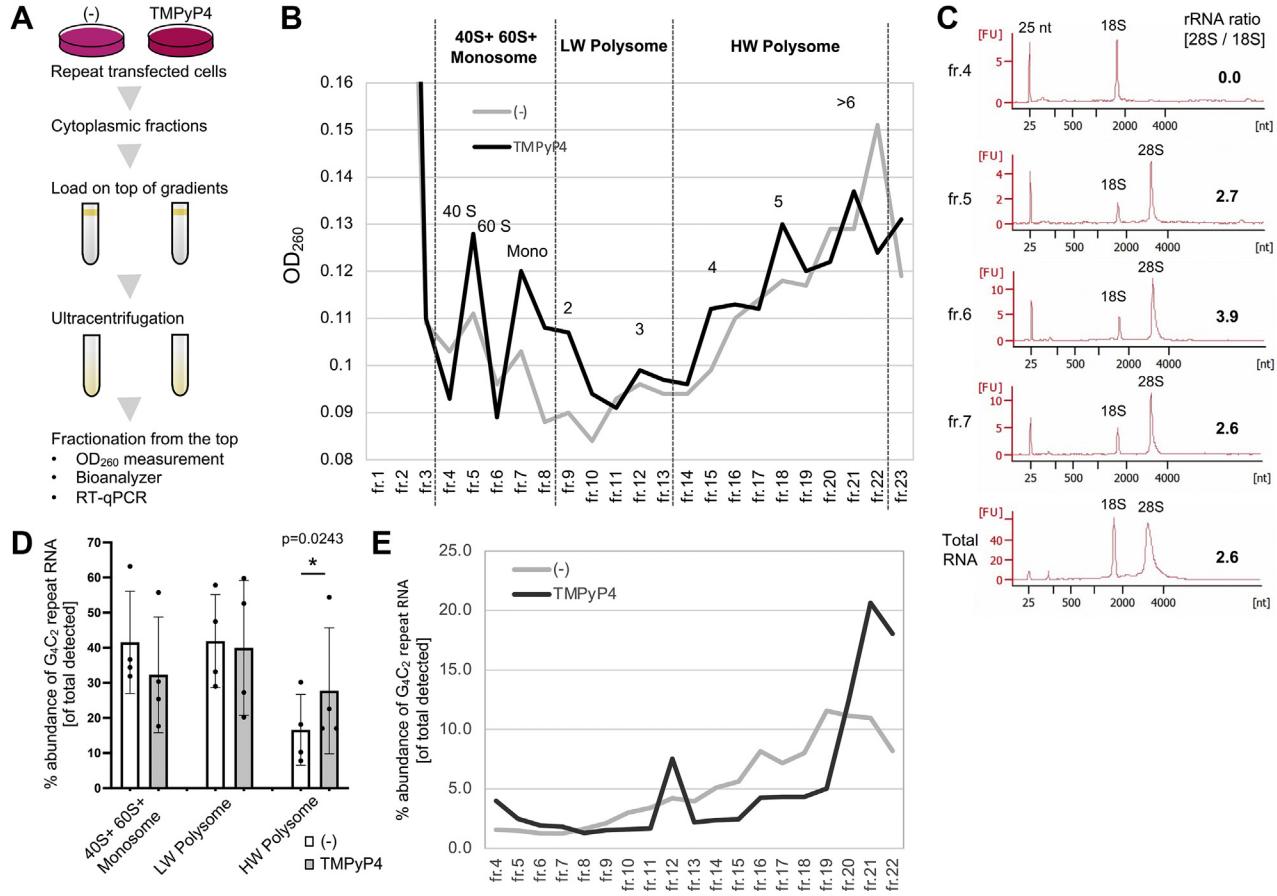

Figure 5. TMPyP4 induces polysome retention on G_4C_2 repeat RNA. *A*, schematic representation of the procedures of polysome profiling assay (see also *Experimental procedures* section). Cytoplasmic fractions from repeat transfected HeLa cells cultured in the presence or the absence of 20 μM TMPyP4 were loaded onto the top of 7 to 47% linear sucrose gradient followed by ultracentrifugation. Fractions (fr.) were successively isolated from the top of the gradient. *B*, representative polysome profiles in $(G_4C_2)_{80}$-transfected HeLa cells treated or not treated with TMPyP4. Fr. 1 to 3 represent nontranslating total RNA (saturating absorbance at 260-nm signal). Fr. 4 to 8 "40S + 60S + monosome" are considered to represent the mRNA containing 40S small ribosome subunit, 60S large ribosome subunit, and monosome. Fr. 9 to 13 "low-weight (LW) polysome" and fr. 14 to 22 "high-weight (HW) polysome" are estimated to be enriched in the signal from two to three (LW) or four or more (HW) ribosome containing mRNA. *C*, electropherograms of bioanalyzer analysis of RNA purified from fr. 4 to fr. 7 of nontreated cells and total RNA from HeLa cells. rRNA ratio (28S/18S) is automatically calculated from each electropherogram. 25-nucleotide (nt) peak represents a supplemented size marker. *D*, RT-quantitative PCR analysis of each of the combined 40S + 60S + monosome, LW polysome, and HW polysome fractions for G_4C_2 repeat RNA. Repeat RNA signals are normalized with spiked EGFP signals by using ΔΔCT method. Graphs are shown as mean ± SD. Each dot represents single data point. Vertical axis is shown as abundance of G_4C_2 repeat RNA (percent of total detected [= sum of (the combined 40S + 60S + monosome) + LW polysome + HW polysome]). Four independent experiments. Two-tailed paired *t* test. *E*, representative distributions of repeat RNA signals from the polysome profile of cells treated or untreated with TMPyP4. G_4C_2 repeat RNA signals are normalized with spiked EGFP RNA by using ΔΔCT method. Vertical axis is shown as percent abundance of repeat RNA (of total detected [fr. 4–22]). EGFP, enhanced GFP; G_4C_2, GGGGCC.

Mechanistically, TMPyP4 induced retention of G_4C_2 repeat RNA in high-weight polysome fraction while inhibiting repeat translation. This suggests slower ribosome runoff and the retention of multiple ribosomes (58) on repeat RNA. Urea-resistant rigid interaction between TMPyP4 and repeat RNA presumably caused ribosome stalling on repeat RNA. Our finding that TMPyP4 target elongation but not initiation of G_4C_2 RAN translation is fully compatible with previous reports describing that *C9orf72* RAN translation initiates at near cognate codons in the 5′ proximal region (*i.e.*, outside) of G_4C_2 repeat (42–45), and TMPyP4 preferentially interacts with RNA G_4C_2 repeat sequence through G-quadruplex structure (52, 62, 63).

Collectively, our results provide evidence that TMPyP4 selectively inhibits elongation of expanded G_4C_2 repeat translation by inducing ribosome stalling. Rigid interaction between TMPyP4 and G_4C_2 repeat RNA could underlie inefficient ribosome runoff. TMPyP4 has multiple targets with latent cytotoxicity, thus may not be suitable for chronic treatment of neurodegenerative patients (64). Nevertheless, compounds more specifically and strongly bind to repeat RNA could have therapeutic potential against repeat-associated diseases including *C9orf72*-FTLD/ALS by inhibiting repeat translation during the elongation step.

Experimental procedures

Cell culture

HeLa cells were cultured in Dulbecco's modified Eagle's medium containing 10% fetal calf serum and penicillin/streptomycin.

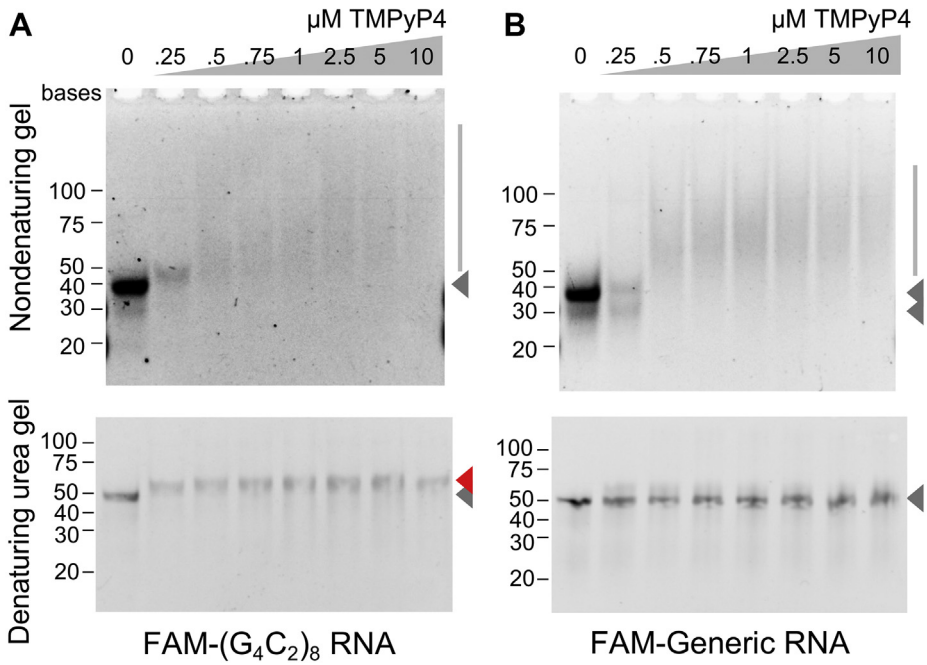

Figure 6. TMPyP4 induces urea-resistant electromobility shift on G_4C_2 repeat RNA. *A*, EMSAs for FAM-labeled synthetic $(G_4C_2)_8$ repeat RNA premixed with increasing concentrations of TMPyP4. RNA–TMPyP4 mixtures were run on nondenaturing 10% TBE gel (*upper panel*) or denaturing 15% TBE gel containing 6.5 M urea (*lower panel*). *B*, EMSA for FAM-labeled generic RNA premixed with increasing concentrations of TMPyP4. The mixtures were run on nondenaturing 10% TBE gel (*upper panel*) or denaturing 15% TBE gel containing 6.5 M urea (*lower panel*). Three independent experiments. G_4C_2, GGGGCC.

Plasmids

The EF1 or CMV-driven $(G_4C_2)_{80}$ expression vectors are previously described (38). Briefly, the vector expresses 80 GGGGCC repeats under the control of the EF1 or CMV promoter including 113 bp of the 5′ flanking region of the human *C9orf72* GGGGCC repeat. The 5′ flanking region contains multiple stop codons in each reading frame and lacks an ATG initiation codon but contain near cognate CUG codon in the poly-GA reading frame (10, 38). A control vector lacking the G_4C_2 repeats (Del Rp) was deleted in a two-step PCR protocol and then subcloned into BamHI/XbaI site of the same vector (38). To insert kozak-ATG in poly-GA reading frame, synthetic oligos 5′-CGCGTTGCCCATGGTGGCTCTAGA-3′ and 5′-CGCGTCTAGAGCCACCATGGGCAA-3′ were annealed and then ligated into BssHII site of the pEF6-$(G_4C_2)_{80}$ vector (ATG-$(G_4C_2)_{80}$). Repeat length was verified with restriction enzyme digestion/electrophoresis upon each preparation of the repeat constructs. The pEF6-EGFP vector was obtained by exchanging the BamHI/NotI fragment of the $(G_4C_2)_{80}$ vector (corresponding 5′ flanking region and repeat region) with the EGFP coding sequence including a Kozak sequence and an ATG start codon (pEF6-EGFP). Sequence was verified with Sanger sequencing.

Antibodies and reagent

The following antibodies were used for Western blot (WB) and dot blot analyses: anti-DYKDDDDK(FLAG) Tag (Cell Signaling; #2368S) WB 1/1000 or anti-FLAG (M2) antibody (Sigma; M1804) WB 1/10,000, anti-GFP clone N86/8 (Neuromab) WB 1/3000 or clone B2 (Santa Cruz) WB 1/500, anti-β-actin (Sigma) WB 1/2000 or 1/3000, and anti-puromycin 12D10 (EMD Millipore) WB 1/25,000. Following reagents were used: TMPyP4 (calbiochem; 613560, CAS 36951-72-1), and CHX (Nakarai Tesque 06741-91; CAS 66-81-9).

RT-qPCR

Total RNA was prepared using the RNeasy and Qiashredder kit (Qiagen). RNA preparations were treated with Turbo DNA-free kit (Thermo Fisher Scientific) to minimize residual DNA contamination. Two micrograms of RNA were used for RT with M-MLV Reverse Transcriptase (Promega) using oligo-(dT) 12 to 18 primer (Invitrogen). RT-qPCR was performed using the 7500 Fast Real-Time PCR System (Applied Biosystems) or ViiA7 Real-Time PCR System (Applied Biosystems) with TaqMan technology. Primers and probes were designed (IDT) for 3′ TAG region of repeat constructs (repeat TAG primer) and EGFP. Repeat TAG, primer 1: TCT CAA ACT GGG ATG CGT AC, primer 2: GTA GTC AAG CGT AGT CTG GG, probe/56-FAM/TG CAG ATA T/Zen/C CAG CAC AGT GGC G/3IABkFQ/(38). EGFP, primer 1: GCA CAA GCT GGA GTA CAA CTA, primer 2: TGT TGT GGC GGA TCT TGA A, probe/56-FAM/AG CAG AAG A/Zen/A CGG CAT CAA GGT GA/3IABkFQ/ (38). Primer/probe sets for human GAPDH, 4326317E (Applied Biosystems), or human ACTB (β-actin), Hs.PT.39a.22214847 (IDT) were used as endogenous control. Each sample was paired with no RT controls showing <1/2^10 (ΔCT >10) signal when compared with reverse transcribed samples, thus excluding contamination of plasmid DNA–derived signal. Each biological sample

was analyzed in duplicate or triplicate. Signals of repeat RNA were normalized to GAPDH or β-actin according to the ΔΔCT method.

Nucleocytoplasmic separation of RNA

Separation of cytoplasmic and nuclear RNA was performed by using PARIS Kit (AM1921; Thermo Fisher Scientific). pEF6-$(G_4C_2)_{80}$-transfected HeLa cells were cultured in the presence or the absence of 20 μM TMPyP4 in 10-cm dish format. About 7.5×10^5 cells were lysed using cell fractionation buffer contained in the kit. After centrifugation at 500*g* at 4 °C for 1 min, the supernatant is termed cytoplasmic fraction and the pellet is called nuclear fraction. After single wash with cell fractionation buffer, nuclear fraction was lysed with cell disruption buffer contained in the PARIS kit. About 5 pg of *in vitro*–transcribed EGFP RNA was added to each fraction as internal control. Subsequent purification procedures were performed as described in the manufacturer's protocol to obtain purified cytoplasmic and nuclear RNA. RNA preparations were treated with Turbo DNA-free kit to minimize residual DNA contamination. RT was performed as described previously but using both random hexamer and oligo-dT primer. RT-qPCR assays targeting GAPDH, β-actin, repeat TAG, and EGFP were performed. Human MALAT1 Hs.PT.58.26451167.g (IDT) was included as a marker for a nuclear-enriched RNA transcript. Signals of MALAT1, GAPDH, β-actin, and repeat RNA in cytoplasm- and nuclear-enriched fractions were normalized to EGFP according to the ΔΔCT method. Total RNA signal is calculated as the sum of signals from cytoplasmic and nuclear RNA–enriched fractions.

Puromycin incorporation assay

Puromycin incorporation assay (alternatively called SUnSET assay) was performed according to Schmidt *et al.* (57). HeLa cells were pretreated with or without 10 or 20 μM of TMPyP4 or 1 or 20 μM of CHX for 20 min followed by additional treatment in the presence or the absence of 10 μg/ml puromycin (Nakarai Tesque; 14861-71) for 10 min for pulse labeling of ongoing translation. Cells were washed once with PBS and then served for WB.

Dot blot analysis

Cells cultured in 12-well plates were lysed with 600 μl of lysis buffer (25 mM Hepes, pH 7.6, 150 mM NaCl, 3% SDS, 0.5% sodium deoxycholate, 1% Triton X-100) supplemented with protease inhibitor cocktail (Sigma) for 10 min and passed through 27G needle for 10 times. The lysates were further diluted 1:5 or 1:25 with the lysis buffer. Hundred microliters of each sample were filtered through a nitrocellulose membrane (0.20-μm pore). The membrane was subsequently boiled in PBS for 10 min, washed once with Tris-buffered saline with Tween-20, and then blocked in I-Block/PBS/TX100. Levels of each DPR were analyzed with antibodies against FLAG tag. Quantified signals from three independent cell culture experiments are shown as fold expression. Signals from corresponding mock transfection were subtracted from signals from DPR expression as nonspecific background.

In vitro *transcription and translation assays*

In vitro transcription and translation assays were performed according to the protocol of Green *et al.* (43) with modification. Briefly, pEF6-based del Rp, $(G_4C_2)_{80}$, ATG-$(G_4C_2)_{80}$, and EGFP vectors linearized with PmeI and were used as templates for *in vitro* transcription with HiScribe T7 high-yield RNA synthesis kit (New England Biolabs; E2040S) according to the manufacturer's protocol. To attach 5′ cap, 3′-O-Me-m7GpppG antireverse cap analog (ARCA) (New England Biolabs; S1411) was added at 8:1 ratio of cap analogue to GTP. The reaction mixtures were incubated at 37 °C for 2 h and then treated with RQ1 RNase-free DNase (Promega) at 37 °C for 15 min. DNase-treated synthetic RNA was then polyadenylated with *Escherichia coli* poly(A) polymerase (New England Biolabs; M0276) for 30 min at 37 °C. The polyadenylated 5′capped RNA was then purified with RNA clean and concentrator-25 kit (Zymo Research). Concentrations of each RNA were estimated from an absorbance at 260 nm and base compositions of *in vitro*–transcribed RNA sequences. Quality of the synthesized RNA was evaluated with 2.2 M formaldehyde—2.5% of agarose gel electrophoresis with RNA century-plus markers (AM7145; Ambion). Flexi Rabbit Reticulocyte Lysate System (Promega; L4540) was used for *in vitro* translation reaction. To facilitate intermolecular interactions between RNA and TMPyP4, 50 ng of transcribed RNA and indicated concentrations of TMPyP4 were preincubated prior to addition of translation reaction mixture. Translation reaction was performed in the presence of 100 mM KCl, 0.5 mM MgOAc, 10 μM minus leucine and 10 μM minus cysteine amino acid mixtures, 1 U/μl of murine RNase inhibitor (New England Biolab; M0314S), and 30% rabbit reticulocyte lysate. Each reaction was performed in a scale of 10 μl at 30 °C for 30 min. After the reaction, samples were treated with 5 μg (=0.5 μl) RNase (Sigma; R6513A; dissolved in ultrapure water [10 mg/ml]) at 30 °C for 5 min and then served for WB.

Polysome profiling assay

To determine whether TMPyP4 induce ribosomal stalling on repeat RNA, polysome profiling analysis according to Pringles *et al.* (59) was performed with modification. About 80 repeats of G_4C_2 repeat transfected HeLa cells were cultured overnight in the presence or the absence of 20 μM TMPyP4 and then treated with 100 μg/ml CHX in PBS for 3 min at 37 °C to halt elongation. Cells were immediately washed, collected, lysed in low-salt lysis buffer (20 mM Tris–HCl, pH 7.4, 50 mM KCl, 10 mM $MgCl_2$, 1% Triton X-100, 0.5% [w/v] sodium deoxycholate, 1 mM 1,4-DTT, 1× Halt protease and phosphatase inhibitor, EDTA free (Thermo; 78442), 100 μg/ml CHX) in the presence of RiboLock RNase inhibitor (Thermo; EO0381) on ice for 10 min. Nuclei were removed by centrifugation at 2000*g* for 5 min. Five hundred microliter of cytoplasmic fraction was then loaded on the top of the 7 to 47% linear sucrose gradient in low-salt buffer (20 mM Tris–HCl,

pH 7.4, 50 mM KCl, 10 mM $MgCl_2$, and 100 μg/ml CHX) formed by gradient master (Biocomp) in a open top centrifuge tube (7030 SETON Scientific). Then ultracentrifugation was performed at 260,808*g* (= 39,000 rpm o the SW41 rotor; L-90K ultracentrifuge [Beckman Coulter]) with slow acceleration up to top speed, 90 min centrifugation at top speed, maximum deceleration until the rotor reaches 2000 rpm, and then no brakes until the rotor automatically stops. After the ultracentrifugation, 500 μl of fractions were sequentially isolated from the top of the gradient by piston gradient fractionator (Biocomp). Since continuous UV monitoring system was not available in our facility, each fraction was measured at an absorbance of 260 nm to monitor polysome profiles. Part of gradient fractions 4 to 7 from TMPyP4-nontreated cells was served for bioanalyzer analysis (described later) to estimate the distribution of 40S, 60S subunits and monosome based on automatically calculated rRNA ratio. The 40S + 60S + monosome (fr. 4–8), low-weight polysome (fr. 9–13), and high-weight polysome (fr. 14–22) fractions were combined, respectively, and proportional amounts of *in vitro*–synthesized EGFP RNA were supplemented as purification controls. Then RNA was purified with TRIzol reagent (Thermo Fisher Scientific) followed by RT-qPCR. RT was performed using both random hexamer and oligo-dT primer. EGFP signal was used as internal control, and relative amount of repeat RNA was calculated with ΔΔCT method. Relative abundance of repeat RNA in the combined 40S + 60S + monosome, low-weight polysomes, and high-weight polysomes were expressed as percent of total fractions (*i.e.*, the combined 40S + 60S + monosome + low-weight polysome + high-weight polysome fractions). To monitor the distribution of the G_4C_2 repeat RNA in TMPyP4-treated or TMPyP4-nontreated cells, fr. 4 to 22 were spiked with equal amount of *in vitro*–synthesized EGFP RNA. Total RNA from these fractions were purified using TRIzol reagent, reverse transcribed, and analyzed with RT-qPCR targeting G_4C_2 repeat RNA (repeat TAG) normalized with EGFP RNA by using ΔΔCT method. Relative abundance of repeat RNA in each fraction was expressed as percent of the sum of signals from fr. 4 to 22.

Bioanalyzer analysis

RNA contained in each fraction (fr. 4–7) of the sucrose gradient analysis of control-treated HeLa cells was purified with the RNA clean and concentrator-25 kit. These RNA and total RNA from HeLa cells were then analyzed with agilent 2100 bioanalyzer system (Agilent) with RNA 6000 Pico Assay kit (Agilent). Data were analyzed with Agilent 2100 expert software (Agilent), and rRNA ratio (28S/18S) was automatically calculated.

EMSA

The 48-nt $(G_4C_2)_8$ repeat: FAM-GGGGCCGGGGCCGGGGCCGGGGCCGGGGCCGGGGC-CGGGGCCGGGGCC and the 49-nt generic (control) RNA oligonucleotides: FAM-AUGCAUCUAGAGGGCCCUA UUCUAUAGUGUCACCUAAAUGCUAGAGCUC were synthesized and HPLC purified (FASMAC) (36, 60, 61). Synthetic RNA oligonucleotides were resolved at the concentration of 10 μM in RNase-free 10 mM Tris–HCl (pH 8.0) with 50 mM KCl. To denature the structure of the RNA, the RNA mixtures were incubated at 80 °C for 3 min and then cooled down to room temperature for 5 min to let the RNA oligonucleotides form their intrinsic tertiary structures. Then indicated concentrations of TMPyP4 were added. About ten volumes of samples were incubated and shaken at 37 °C for 5 min followed by the addition of one volume of 0.5% glycerol containing bromophenol blue as DNA-loading buffer. Samples were immediately applied to 10% TBE gel (nondenaturing gel; EC6275BOX; Invitrogen) or self-made 6.5 M urea and 15% TBE gel (denaturing gel). Prestain marker for small RNA plus (DynaMaker; DM253) was used as RNA size marker. Electrophoresis was carried out at 180 V for 50 min. Fluorescent signals were obtained with LAS3000 imager (Fujifilm).

Statistics

Statistical analysis was performed using Prism 9 (GraphPad Software, Inc) or JMP Pro 14 software (SAS Institute Inc).

Data availability

All data are included within the article.

Acknowledgments—We thank Drs Yoshihiro Nihei, Tesshin Miyamoto, Kanta Yanagida, and Takashi Morihara for helpful discussion as well as Katsutoshi Niwa and Saki Ishino (Center for Medical Research and Education, Graduate School of Medicine, Osaka University) for their technical assistance on polysome profiling assay.

Author contributions—K. M. and C. H. conceptualization; K. M., Y. K., S. T., F. K., B. N., D. E., and Y. N. methodology; K. M., S. G., T. Y., and R. U. validation; K. M. formal analysis; K. M., S. G., T. Y., and R. U. investigation; K. M. data curation; K. M. writing–original draft; K. M., D. E., and Y. N. writing–review and editing; K. M. and S. G. visualization; K. M., D. E., C. H., Y. N., and M. I. supervision; K. M. project administration; K. M., S. T., C. H., and Y. N. funding acquisition.

Funding and additional information—This work was supported by the Japan Society for the Promotion of Science KAKENHI grant number JP16H06953 (to K. M.), JP17H05091 (to K. M.), JP18K19515 (to K. M.), JP20H03602 (to K. M.), JP20H05927 (to K. M. and Y. N.), Japan Agency for Medical Research and Development under grant number JP20ek0109316 (to K. M. and Y. N.), JST FOREST Program under grant number JPMJFR200Z (to K. M.), SENSHIN Medical Research Foundation (to K. M. and S. T.), Mochida Memorial Foundation (to K. M.) and Takeda Science Foundation (to K. M.), the European Research Council under the European Union's Seventh Framework Program (FP7/2007-2013)/ERC grant agreement no. 617198 (DPR-MODELS to D. E.). C. H. is supported by the Deutsche Forschungsgemeinschaft (German Research Foundation) under Germany's Excellence Strategy within the framework of the Munich Cluster for Systems Neurology (EXC 2145 SyNergy; ID: 390857198) and the Nomis Foundation.

Conflict of interest—The authors declare that they have no conflicts of interest with the contents of this article.

Abbreviations—The abbreviations used are: ALS, amyotrophic lateral sclerosis; CHX, cycloheximide; CMV, cytomegalovirus; DPR, dipeptide repeat; EF1, elongation factor 1; EGFP, enhanced GFP; FAM, fluorescein; fr., fraction; FTLD, frontotemporal lobar degeneration; GA, glycine alanine; G_4C_2, GGGGCC; GP, glycine proline; GR, glycine arginine; qPCR, quantitative PCR; RAN, *r*epeat-*a*ssociated *n*on-AUG; WB, Western blot.

References

1. Renton, A. E., Majounie, E., Waite, A., Simon-Sanchez, J., Rollinson, S., Gibbs, J. R., Schymick, J. C., Laaksovirta, H., van Swieten, J. C., Myllykangas, L., Kalimo, H., Paetau, A., Abramzon, Y., Remes, A. M., Kaganovich, A., *et al.* (2011) A hexanucleotide repeat expansion in C9ORF72 is the cause of chromosome 9p21-linked ALS-FTD. *Neuron* **72**, 257–268
2. Gijselinck, I., Van Langenhove, T., van der Zee, J., Sleegers, K., Philtjens, S., Kleinberger, G., Janssens, J., Bettens, K., Van Cauwenberghe, C., Pereson, S., Engelborghs, S., Sieben, A., De Jonghe, P., Vandenberghe, R., Santens, P., *et al.* (2012) A C9orf72 promoter repeat expansion in a Flanders-Belgian cohort with disorders of the frontotemporal lobar degeneration-amyotrophic lateral sclerosis spectrum: A gene identification study. *Lancet Neurol.* **11**, 54–65
3. DeJesus-Hernandez, M., Mackenzie, I. R., Boeve, B. F., Boxer, A. L., Baker, M., Rutherford, N. J., Nicholson, A. M., Finch, N. A., Flynn, H., Adamson, J., Kouri, N., Wojtas, A., Sengdy, P., Hsiung, G. Y., Karydas, A., *et al.* (2011) Expanded GGGGCC hexanucleotide repeat in noncoding region of C9ORF72 causes chromosome 9p-linked FTD and ALS. *Neuron* **72**, 245–256
4. Lee, Y. B., Chen, H. J., Peres, J. N., Gomez-Deza, J., Attig, J., Stalekar, M., Troakes, C., Nishimura, A. L., Scotter, E. L., Vance, C., Adachi, Y., Sardone, V., Miller, J. W., Smith, B. N., Gallo, J. M., *et al.* (2013) Hexanucleotide repeats in ALS/FTD form length-dependent RNA foci, sequester RNA binding proteins, and are neurotoxic. *Cell Rep.* **5**, 1178–1186
5. Mori, K., Lammich, S., Mackenzie, I. R., Forne, I., Zilow, S., Kretzschmar, H., Edbauer, D., Janssens, J., Kleinberger, G., Cruts, M., Herms, J., Neumann, M., Van Broeckhoven, C., Arzberger, T., and Haass, C. (2013) hnRNP A3 binds to GGGGCC repeats and is a constituent of p62-positive/TDP43-negative inclusions in the hippocampus of patients with C9orf72 mutations. *Acta Neuropathol.* **125**, 413–423
6. Cooper-Knock, J., Walsh, M. J., Higginbottom, A., Robin Highley, J., Dickman, M. J., Edbauer, D., Ince, P. G., Wharton, S. B., Wilson, S. A., Kirby, J., Hautbergue, G. M., and Shaw, P. J. (2014) Sequestration of multiple RNA recognition motif-containing proteins by C9orf72 repeat expansions. *Brain* **137**, 2040–2051
7. Ash, P. E., Bieniek, K. F., Gendron, T. F., Caulfield, T., Lin, W. L., Dejesus-Hernandez, M., van Blitterswijk, M. M., Jansen-West, K., Paul, J. W., 3rd, Rademakers, R., Boylan, K. B., Dickson, D. W., and Petrucelli, L. (2013) Unconventional translation of C9ORF72 GGGGCC expansion generates insoluble polypeptides specific to c9FTD/ALS. *Neuron* **77**, 639–646
8. Gendron, T. F., Bieniek, K. F., Zhang, Y. J., Jansen-West, K., Ash, P. E., Caulfield, T., Daughrity, L., Dunmore, J. H., Castanedes-Casey, M., Chew, J., Cosio, D. M., van Blitterswijk, M., Lee, W. C., Rademakers, R., Boylan, K. B., *et al.* (2013) Antisense transcripts of the expanded C9ORF72 hexanucleotide repeat form nuclear RNA foci and undergo repeat-associated non-ATG translation in c9FTD/ALS. *Acta Neuropathol.* **126**, 829–844
9. Mori, K., Arzberger, T., Grasser, F. A., Gijselinck, I., May, S., Rentzsch, K., Weng, S. M., Schludi, M. H., van der Zee, J., Cruts, M., Van Broeckhoven, C., Kremmer, E., Kretzschmar, H. A., Haass, C., and Edbauer, D. (2013) Bidirectional transcripts of the expanded C9orf72 hexanucleotide repeat are translated into aggregating dipeptide repeat proteins. *Acta Neuropathol.* **126**, 881–893
10. Mori, K., Weng, S. M., Arzberger, T., May, S., Rentzsch, K., Kremmer, E., Schmid, B., Kretzschmar, H. A., Cruts, M., Van Broeckhoven, C., Haass, C., and Edbauer, D. (2013) The C9orf72 GGGGCC repeat is translated into aggregating dipeptide-repeat proteins in FTLD/ALS. *Science* **339**, 1335–1338
11. Zu, T., Liu, Y., Banez-Coronel, M., Reid, T., Pletnikova, O., Lewis, J., Miller, T. M., Harms, M. B., Falchook, A. E., Subramony, S. H., Ostrow, L. W., Rothstein, J. D., Troncoso, J. C., and Ranum, L. P. (2013) RAN proteins and RNA foci from antisense transcripts in C9ORF72 ALS and frontotemporal dementia. *Proc. Natl. Acad. Sci. U. S. A.* **110**, E4968–4977
12. Zu, T., Gibbens, B., Doty, N. S., Gomes-Pereira, M., Huguet, A., Stone, M. D., Margolis, J., Peterson, M., Markowski, T. W., Ingram, M. A., Nan, Z., Forster, C., Low, W. C., Schoser, B., Somia, N. V., *et al.* (2011) Non-ATG-initiated translation directed by microsatellite expansions. *Proc. Natl. Acad. Sci. U. S. A.* **108**, 260–265
13. Mackenzie, I. R., Arzberger, T., Kremmer, E., Troost, D., Lorenzl, S., Mori, K., Weng, S. M., Haass, C., Kretzschmar, H. A., Edbauer, D., and Neumann, M. (2013) Dipeptide repeat protein pathology in C9ORF72 mutation cases: Clinico-pathological correlations. *Acta Neuropathol.* **126**, 859–879
14. Mackenzie, I. R., Frick, P., Grasser, F. A., Gendron, T. F., Petrucelli, L., Cashman, N. R., Edbauer, D., Kremmer, E., Prudlo, J., Troost, D., and Neumann, M. (2015) Quantitative analysis and clinico-pathological correlations of different dipeptide repeat protein pathologies in C9ORF72 mutation carriers. *Acta Neuropathol.* **130**, 845–861
15. Mann, D. M., Rollinson, S., Robinson, A., Bennion Callister, J., Thompson, J. C., Snowden, J. S., Gendron, T., Petrucelli, L., Masuda-Suzukake, M., Hasegawa, M., Davidson, Y., and Pickering-Brown, S. (2013) Dipeptide repeat proteins are present in the p62 positive inclusions in patients with frontotemporal lobar degeneration and motor neurone disease associated with expansions in C9ORF72. *Acta Neuropathol. Commun.* **1**, 68
16. Gendron, T. F., Chew, J., Stankowski, J. N., Hayes, L. R., Zhang, Y. J., Prudencio, M., Carlomagno, Y., Daughrity, L. M., Jansen-West, K., Perkerson, E. A., O'Raw, A., Cook, C., Pregent, L., Belzil, V., van Blitterswijk, M., *et al.* (2017) Poly(GP) proteins are a useful pharmacodynamic marker for C9ORF72-associated amyotrophic lateral sclerosis. *Sci. Transl. Med.* **9**, eaai7866
17. Lehmer, C., Oeckl, P., Weishaupt, J. H., Volk, A. E., Diehl-Schmid, J., Schroeter, M. L., Lauer, M., Kornhuber, J., Levin, J., Fassbender, K., Landwehrmeyer, B., German Consortium for Frontotemporal Lobar Degeneration, Schludi, M. H., Arzberger, T., Kremmer, E., *et al.* (2017) Poly-GP in cerebrospinal fluid links C9orf72-associated dipeptide repeat expression to the asymptomatic phase of ALS/FTD. *EMBO Mol. Med.* **9**, 859–868
18. Saberi, S., Stauffer, J. E., Jiang, J., Garcia, S. D., Taylor, A. E., Schulte, D., Ohkubo, T., Schloffman, C. L., Maldonado, M., Baughn, M., Rodriguez, M. J., Pizzo, D., Cleveland, D., and Ravits, J. (2018) Sense-encoded poly-GR dipeptide repeat proteins correlate to neurodegeneration and uniquely co-localize with TDP-43 in dendrites of repeat-expanded C9orf72 amyotrophic lateral sclerosis. *Acta Neuropathol.* **135**, 459–474
19. Quaegebeur, A., Glaria, I., Lashley, T., and Isaacs, A. M. (2020) Soluble and insoluble dipeptide repeat protein measurements in C9orf72-frontotemporal dementia brains show regional differential solubility and correlation of poly-GR with clinical severity. *Acta Neuropathol. Commun.* **8**, 184
20. Sakae, N., Bieniek, K. F., Zhang, Y. J., Ross, K., Gendron, T. F., Murray, M. E., Rademakers, R., Petrucelli, L., and Dickson, D. W. (2018) Poly-GR dipeptide repeat polymers correlate with neurodegeneration and clinicopathological subtypes in C9ORF72-related brain disease. *Acta Neuropathol. Commun.* **6**, 63
21. Gittings, L. M., Boeynaems, S., Lightwood, D., Clargo, A., Topia, S., Nakayama, L., Troakes, C., Mann, D. M. A., Gitler, A. D., Lashley, T., and Isaacs, A. M. (2020) Symmetric dimethylation of poly-GR correlates with disease duration in C9orf72 FTLD and ALS and reduces poly-GR phase separation and toxicity. *Acta Neuropathol.* **139**, 407–410
22. Chew, J., Gendron, T. F., Prudencio, M., Sasaguri, H., Zhang, Y. J., Castanedes-Casey, M., Lee, C. W., Jansen-West, K., Kurti, A., Murray, M. E.,

Bieniek, K. F., Bauer, P. O., Whitelaw, E. C., Rousseau, L., Stankowski, J. N., *et al.* (2015) C9ORF72 repeat expansions in mice cause TDP-43 pathology, neuronal loss, and behavioral deficits. *Science* **348**, 1151–1154
23. Liu, Y., Pattamatta, A., Zu, T., Reid, T., Bardhi, O., Borchelt, D. R., Yachnis, A. T., and Ranum, L. P. (2016) C9orf72 BAC mouse model with motor deficits and neurodegenerative features of ALS/FTD. *Neuron* **90**, 521–534
24. Tran, H., Almeida, S., Moore, J., Gendron, T. F., Chalasani, U., Lu, Y., Du, X., Nickerson, J. A., Petrucelli, L., Weng, Z., and Gao, F. B. (2015) Differential toxicity of nuclear RNA foci versus dipeptide repeat proteins in a Drosophila model of C9ORF72 FTD/ALS. *Neuron* **87**, 1207–1214
25. May, S., Hornburg, D., Schludi, M. H., Arzberger, T., Rentzsch, K., Schwenk, B. M., Grasser, F. A., Mori, K., Kremmer, E., Banzhaf-Strathmann, J., Mann, M., Meissner, F., and Edbauer, D. (2014) C9orf72 FTLD/ALS-associated Gly-Ala dipeptide repeat proteins cause neuronal toxicity and Unc119 sequestration. *Acta Neuropathol.* **128**, 485–503
26. Mizielinska, S., Gronke, S., Niccoli, T., Ridler, C. E., Clayton, E. L., Devoy, A., Moens, T., Norona, F. E., Woollacott, I. O., Pietrzyk, J., Cleverley, K., Nicoll, A. J., Pickering-Brown, S., Dols, J., Cabecinha, M., *et al.* (2014) C9orf72 repeat expansions cause neurodegeneration in Drosophila through arginine-rich proteins. *Science* **345**, 1192–1194
27. Zhang, Y. J., Gendron, T. F., Grima, J. C., Sasaguri, H., Jansen-West, K., Xu, Y. F., Katzman, R. B., Gass, J., Murray, M. E., Shinohara, M., Lin, W. L., Garrett, A., Stankowski, J. N., Daughrity, L., Tong, J., *et al.* (2016) C9ORF72 poly(GA) aggregates sequester and impair HR23 and nucleocytoplasmic transport proteins. *Nat. Neurosci.* **19**, 668–677
28. Schludi, M. H., Becker, L., Garrett, L., Gendron, T. F., Zhou, Q., Schreiber, F., Popper, B., Dimou, L., Strom, T. M., Winkelmann, J., von Thaden, A., Rentzsch, K., May, S., Michaelsen, M., Schwenk, B. M., *et al.* (2017) Spinal poly-GA inclusions in a C9orf72 mouse model trigger motor deficits and inflammation without neuron loss. *Acta Neuropathol.* **134**, 241–254
29. Wen, X., Tan, W., Westergard, T., Krishnamurthy, K., Markandaiah, S. S., Shi, Y., Lin, S., Shneider, N. A., Monaghan, J., Pandey, U. B., Pasinelli, P., Ichida, J. K., and Trotti, D. (2014) Antisense proline-arginine RAN dipeptides linked to C9ORF72-ALS/FTD form toxic nuclear aggregates that initiate *in vitro* and *in vivo* neuronal death. *Neuron* **84**, 1213–1225
30. Yamakawa, M., Ito, D., Honda, T., Kubo, K., Noda, M., Nakajima, K., and Suzuki, N. (2015) Characterization of the dipeptide repeat protein in the molecular pathogenesis of c9FTD/ALS. *Hum. Mol. Genet.* **24**, 1630–1645
31. Lee, Y. B., Baskaran, P., Gomez-Deza, J., Chen, H. J., Nishimura, A. L., Smith, B. N., Troakes, C., Adachi, Y., Stepto, A., Petrucelli, L., Gallo, J. M., Hirth, F., Rogelj, B., Guthrie, S., and Shaw, C. E. (2017) C9orf72 poly GA RAN-translated protein plays a key role in amyotrophic lateral sclerosis via aggregation and toxicity. *Hum. Mol. Genet.* **26**, 4765–4777
32. Khosravi, B., Hartmann, H., May, S., Mohl, C., Ederle, H., Michaelsen, M., Schludi, M. H., Dormann, D., and Edbauer, D. (2017) Cytoplasmic poly-GA aggregates impair nuclear import of TDP-43 in C9orf72 ALS/FTLD. *Hum. Mol. Genet.* **26**, 790–800
33. Kwon, I., Xiang, S., Kato, M., Wu, L., Theodoropoulos, P., Wang, T., Kim, J., Yun, J., Xie, Y., and McKnight, S. L. (2014) Poly-dipeptides encoded by the C9orf72 repeats bind nucleoli, impede RNA biogenesis, and kill cells. *Science* **345**, 1139–1145
34. Guo, Q., Lehmer, C., Martinez-Sanchez, A., Rudack, T., Beck, F., Hartmann, H., Perez-Berlanga, M., Frottin, F., Hipp, M. S., Hartl, F. U., Edbauer, D., Baumeister, W., and Fernandez-Busnadiego, R. (2018) *In Situ* structure of neuronal C9orf72 poly-GA aggregates reveals proteasome recruitment. *Cell* **172**, 696–705.e612
35. Cook, C. N., Wu, Y., Odeh, H. M., Gendron, T. F., Jansen-West, K., Del Rosso, G., Yue, M., Jiang, P., Gomes, E., Tong, J., Daughrity, L. M., Avendano, N. M., Castanedes-Casey, M., Shao, W., Oskarsson, B., *et al.* (2020) C9orf72 poly(GR) aggregation induces TDP-43 proteinopathy. *Sci. Transl. Med.* **12**, eabb3774
36. Kawabe, Y., Mori, K., Yamashita, T., Gotoh, S., and Ikeda, M. (2020) The RNA exosome complex degrades expanded hexanucleotide repeat RNA in C9orf72 FTLD/ALS. *EMBO J.* **39**, e102700
37. Hutten, S., Usluer, S., Bourgeois, B., Simonetti, F., Odeh, H. M., Fare, C. M., Czuppa, M., Hruska-Plochan, M., Hofweber, M., Polymenidou, M., Shorter, J., Edbauer, D., Madl, T., and Dormann, D. (2020) Nuclear import receptors directly bind to arginine-rich dipeptide repeat proteins and suppress their pathological interactions. *Cell Rep.* **33**, 108538
38. Mori, K., Nihei, Y., Arzberger, T., Zhou, Q., Mackenzie, I. R., Hermann, A., Hanisch, F., German Consortium for Frontotemporal Lobar, D, Bavarian Brain Banking, A, Kamp, F., Nuscher, B., Orozco, D., Edbauer, D., and Haass, C. (2016) Reduced hnRNPA3 increases C9orf72 repeat RNA levels and dipeptide-repeat protein deposition. *EMBO Rep.* **17**, 1314–1325
39. Nihei, Y., Mori, K., Werner, G., Arzberger, T., Zhou, Q., Khosravi, B., Japtok, J., Hermann, A., Sommacal, A., Weber, M., German Consortium for Frontotemporal Lobar Degeneration; Bavarian Brain Banking Alliance, Kamp, F., Nuscher, B., Edbauer, D., and Haass, C. (2020) Poly-glycine-alanine exacerbates C9orf72 repeat expansion-mediated DNA damage via sequestration of phosphorylated ATM and loss of nuclear hnRNPA3. *Acta Neuropathol.* **139**, 99–118
40. Shi, Y., Lin, S., Staats, K. A., Li, Y., Chang, W. H., Hung, S. T., Hendricks, E., Linares, G. R., Wang, Y., Son, E. Y., Wen, X., Kisler, K., Wilkinson, B., Menendez, L., Sugawara, T., *et al.* (2018) Haploinsufficiency leads to neurodegeneration in C9ORF72 ALS/FTD human induced motor neurons. *Nat. Med.* **24**, 313–325
41. Zhu, Q., Jiang, J., Gendron, T. F., McAlonis-Downes, M., Jiang, L., Taylor, A., Diaz Garcia, S., Ghosh Dastidar, S., Rodriguez, M. J., King, P., Zhang, Y., La Spada, A. R., Xu, H., Petrucelli, L., Ravits, J., *et al.* (2020) Reduced C9ORF72 function exacerbates gain of toxicity from ALS/FTD-causing repeat expansion in C9orf72. *Nat. Neurosci.* **23**, 615–624
42. Boivin, M., Pfister, V., Gaucherot, A., Ruffenach, F., Negroni, L., Sellier, C., and Charlet-Berguerand, N. (2020) Reduced autophagy upon C9ORF72 loss synergizes with dipeptide repeat protein toxicity in G4C2 repeat expansion disorders. *EMBO J.* **39**, e100574
43. Green, K. M., Glineburg, M. R., Kearse, M. G., Flores, B. N., Linsalata, A. E., Fedak, S. J., Goldstrohm, A. C., Barmada, S. J., and Todd, P. K. (2017) RAN translation at C9orf72-associated repeat expansions is selectively enhanced by the integrated stress response. *Nat. Commun.* **8**, 2005
44. Tabet, R., Schaeffer, L., Freyermuth, F., Jambeau, M., Workman, M., Lee, C. Z., Lin, C. C., Jiang, J., Jansen-West, K., Abou-Hamdan, H., Desaubry, L., Gendron, T., Petrucelli, L., Martin, F., and Lagier-Tourenne, C. (2018) CUG initiation and frameshifting enable production of dipeptide repeat proteins from ALS/FTD C9ORF72 transcripts. *Nat. Commun.* **9**, 152
45. Sonobe, Y., Ghadge, G., Masaki, K., Sendoel, A., Fuchs, E., and Roos, R. P. (2018) Translation of dipeptide repeat proteins from the C9ORF72 expanded repeat is associated with cellular stress. *Neurobiol. Dis.* **116**, 155–165
46. Cheng, W., Wang, S., Mestre, A. A., Fu, C., Makarem, A., Xian, F., Hayes, L. R., Lopez-Gonzalez, R., Drenner, K., Jiang, J., Cleveland, D. W., and Sun, S. (2018) C9ORF72 GGGGCC repeat-associated non-AUG translation is upregulated by stress through eIF2alpha phosphorylation. *Nat. Commun.* **9**, 51
47. Westergard, T., McAvoy, K., Russell, K., Wen, X., Pang, Y., Morris, B., Pasinelli, P., Trotti, D., and Haeusler, A. (2019) Repeat-associated non-AUG translation in C9orf72-ALS/FTD is driven by neuronal excitation and stress. *EMBO Mol. Med.* **11**, e9423
48. Zu, T., Guo, S., Bardhi, O., Ryskamp, D. A., Li, J., Khoramian Tusi, S., Engelbrecht, A., Klippel, K., Chakrabarty, P., Nguyen, L., Golde, T. E., Sonenberg, N., and Ranum, L. P. W. (2020) Metformin inhibits RAN translation through PKR pathway and mitigates disease in C9orf72 ALS/FTD mice. *Proc. Natl. Acad. Sci. U. S. A.* **117**, 18591–18599
49. Cheng, W., Wang, S., Zhang, Z., Morgens, D. W., Hayes, L. R., Lee, S., Portz, B., Xie, Y., Nguyen, B. V., Haney, M. S., Yan, S., Dong, D., Coyne, A. N., Yang, J., Xian, F., *et al.* (2019) CRISPR-Cas9 screens identify the RNA helicase DDX3X as a repressor of C9ORF72 (GGGGCC)n repeat-associated non-AUG translation. *Neuron* **104**, 885–898.e888
50. Fratta, P., Mizielinska, S., Nicoll, A. J., Zloh, M., Fisher, E. M., Parkinson, G., and Isaacs, A. M. (2012) C9orf72 hexanucleotide repeat associated with amyotrophic lateral sclerosis and frontotemporal dementia forms RNA G-quadruplexes. *Sci. Rep.* **2**, 1016

51. Haeusler, A. R., Donnelly, C. J., Periz, G., Simko, E. A., Shaw, P. G., Kim, M. S., Maragakis, N. J., Troncoso, J. C., Pandey, A., Sattler, R., Rothstein, J. D., and Wang, J. (2014) C9orf72 nucleotide repeat structures initiate molecular cascades of disease. *Nature* **507**, 195–200
52. Zamiri, B., Reddy, K., Macgregor, R. B., Jr., and Pearson, C. E. (2014) TMPyP4 porphyrin distorts RNA G-quadruplex structures of the disease-associated r(GGGGCC)n repeat of the C9orf72 gene and blocks interaction of RNA-binding proteins. *J. Biol. Chem.* **289**, 4653–4659
53. Zhang, K., Donnelly, C. J., Haeusler, A. R., Grima, J. C., Machamer, J. B., Steinwald, P., Daley, E. L., Miller, S. J., Cunningham, K. M., Vidensky, S., Gupta, S., Thomas, M. A., Hong, I., Chiu, S. L., Huganir, R. L., *et al.* (2015) The C9orf72 repeat expansion disrupts nucleocytoplasmic transport. *Nature* **525**, 56–61
54. Fay, M. M., Anderson, P. J., and Ivanov, P. (2017) ALS/FTD-Associated C9ORF72 repeat RNA promotes phase transitions in vitro and in cells. *Cell Rep.* **21**, 3573–3584
55. Green, K. M., Sheth, U. J., Flores, B. N., Wright, S. E., Sutter, A. B., Kearse, M. G., Barmada, S. J., Ivanova, M. I., and Todd, P. K. (2019) High-throughput screening yields several small-molecule inhibitors of repeat-associated non-AUG translation. *J. Biol. Chem.* **294**, 18624–18638
56. Simone, R., Balendra, R., Moens, T. G., Preza, E., Wilson, K. M., Heslegrave, A., Woodling, N. S., Niccoli, T., Gilbert-Jaramillo, J., Abdelkarim, S., Clayton, E. L., Clarke, M., Konrad, M. T., Nicoll, A. J., Mitchell, J. S., *et al.* (2018) G-quadruplex-binding small molecules ameliorate C9orf72 FTD/ALS pathology *in vitro* and *in vivo*. *EMBO Mol. Med.* **10**, 22–31
57. Schmidt, E. K., Clavarino, G., Ceppi, M., and Pierre, P. (2009) SUnSET, a nonradioactive method to monitor protein synthesis. *Nat. Methods* **6**, 275–277
58. Saini, P., Eyler, D. E., Green, R., and Dever, T. E. (2009) Hypusine-containing protein eIF5A promotes translation elongation. *Nature* **459**, 118–121
59. Pringle, E. S., McCormick, C., and Cheng, Z. (2019) Polysome profiling analysis of mRNA and associated proteins engaged in translation. *Curr. Protoc. Mol. Biol.* **125**, e79
60. Januszyk, K., Liu, Q., and Lima, C. D. (2011) Activities of human RRP6 and structure of the human RRP6 catalytic domain. *RNA* **17**, 1566–1577
61. Liu, Q., Greimann, J. C., and Lima, C. D. (2006) Reconstitution, activities, and structure of the eukaryotic RNA exosome. *Cell* **127**, 1223–1237
62. Alniss, H., Zamiri, B., Khalaj, M., Pearson, C. E., and Macgregor, R. B., Jr. (2018) Thermodynamic and spectroscopic investigations of TMPyP4 association with guanine- and cytosine-rich DNA and RNA repeats of C9orf72. *Biochem. Biophys. Res. Commun.* **495**, 2410–2417
63. Mulholland, K., Sullivan, H. J., Garner, J., Cai, J., Chen, B., and Wu, C. (2020) Three-dimensional structure of RNA monomeric G-quadruplex containing ALS and FTD related G4C2 repeat and its binding with TMPyP4 probed by homology modeling based on experimental constraints and molecular dynamics simulations. *ACS Chem. Neurosci.* **11**, 57–75
64. Fujiwara, N., Mazzola, M., Cai, E., Wang, M., and Cave, J. W. (2015) TMPyP4, a stabilizer of nucleic acid secondary structure, is a novel acetylcholinesterase inhibitor. *PLoS One* **10**, e0139167